Nickel oxide hollow nano-fiber electrodes for electrochemical capacitors

Satoshi Machida and Hiromori Tsutsumi

Yamaguchi University, 2-16-1 Tokiwadai, Ube, 755-8611, Japan,
tsutsumi@yamaguchi-u.ac.jp

ABSTRACT

Morphology of active materials in electrodes affects electrochemical performance and capacity of energy storage devices. New architectures, for example three-dimensional structure (3D), not a flat film, for electrodes and cells will overcome the traditional electrodes' problems, such as low utilization of active materials, rate limit of ion diffusion. However, preparation of 3D electrodes needs complex, multi-step and high-cost processes. We prepared nickel oxide (NiO) hollow nano-fiber electrodes with the combination of the electrospinning and electroless plating techniques and evaluated their performance as electrodes for electrochemical capacitors. Non-woven mats with poly(methyl methacrylate) (PMMA) nano-fibers were prepared by electrospinning technique. Then the PMMA mats were immersed into the Ni electroless plating bath and the Ni-plated PMMA fibers were heated at 550°C for 4h to remove the PMMA. The average outer diameter of the NiO hollow nano-fibers was 3 μm and inside was 0.67 μm. EDX analysis of the heat treated mats suggested that the follow fibers contain nickel oxide (NiO) with some phosphorous compounds and the PMMA in the mats as a mold is removed completely. The cyclic voltammograms for the NiO hollow nano-fiber electrode in the aqueous solution (1 M KOH) indicated that the electrode is electrochemically active. The estimated capacity of the NiO hollow fiber electrode from the voltammograms was 190.5 F g^{-1} (per gram of NiO).

Keywords: electrospinning, electroless plating, nickel oxide, capacitor, energy storage

1 INTRODUCTION

Energy storage devices, battery or capacitor, have electrodes with active materials for energy storage reaction and electrolytes for ionic conduction. Energy and power density of such energy storage devices depends on energy storage mechanism of active materials, shape of their electrodes, conductivity of electrolytes, and so on. Shape of electrodes in the devices affects the amount of reactive surface area of the electrodes, ion mobility and diffusion in the electrodes,

Dunn, *et al.* have reviewed the emerging area of three-dimensional (3D) batteries [1]. Conventional battery designs with two dimensional (2D) electrode geometries has some problems, which the total amount of stored energy for 2D batteries decreases and the maximum current output falls in small batteries. To overcome such shortcomings, 3D batteries have unique and distinctive architectures. For example, cylinder-shape electrodes with sub-micrometer or nano-meter size have some merits. The concentric arrangement has a 3D electrode array coated by an electrolyte layer with the remaining free volume filled by the other electrode material. This design, originally proposed by Martin [2] not only provides short transport distances between electrodes, it also leads to higher energy densities than those of the interdigitated configuration because of the lower volume fraction occupied by the electrolyte.

We prepared nickel oxide (NiO) hollow nano-fiber electrodes with combination of the electrospinning and electroless plating techniques and evaluated their performance as electrodes for electrochemical capacitors.

2 EXPERIMENTAL

2.1 Materials

All chemicals for this investigation were used as received. Average degree of polymerization of poly(methyl methacrylate), PMMA, was 6,000.

2.2 Preparation of PMMA-based fibers

Equipments for electrospinning process was constructed with a high-voltage power supply (Matsusada precision), a syringe pump (KD Scientific), and a syringe with a needle. The PMMA chloroform solution (5.5 wt. %) containing $PdCl_2$ (*ca.* 0.12 wt. %) was charged into the syringe and then spinning process was started. Applied voltage was 15 kV, the distance between the needle and the stainless steel plate as a collector of non-woven PMMA mat with fine fibers was 10 cm, and the flow rate of the solution was 1ml/h. The average diameter of the resulted PMMA fibers with $PdCl_2$ in the mat was 0.67 μm.

2.3 Nickel Electroless Plating on the PMMA Mats

Nickel (Ni) electroless plating on the electrospun PMMA fibers in the mat was performed as mentioned

following section. The composition of the Ni-P electroless plating bath is listed in Table 1.

Table 1 Composition of electroless nickel plating bath and plating condition

Compound	Weight of compound /g
$NiSO_4 \cdot 6H_2O$	2.9962
$Na_3C_6H_5O_7 \cdot 2H_2O$	1.5886
CH_3COONH_4	2.4650
$NaH_2PO_2 \cdot 2H_2O$	2.3325
water	100

The bath pH was 6 and temperature was 60°C.

The PMMA mats were immersed into the electroless plating bath for 30, 60, or 120 minutes, washed with pure water after the plating process, and dried.

2.4 Thermal Treatment of Nickel-plated PMMA fibers

The resulted fibers were treated with a muffle furnace (FO-100, Yamamto Scientific Co.) at 400°C or 550°C for 2 or 4 hours in the air. Structure and chemical composition of the heat treated fibers were determined with SEM observation, EDX analysis, and XRD measurements.

2.5 Measurements

Observation of the electrospun fibers, the Ni plated fibers and heat-treated fibers were performed with a digital microscope (VH-5000, VH-Z450, Keyence) and an SEM (VE-9800, Keyence). Their structural characterization was made using an X-ray diffractometer with filtered CuKα radiation (XRD-D1, Shimadzu). Elemental analysis on the surface of the fibers was performed with an EDX technique (Genesis 2000). Electrochemical responses of the Ni hollow fiber electrodes were checked in an alkali-aqueous solution (1 M KOH) with a conventional three-electrode cell and a computer-controlled electrochemical response analyzer (HZ-3000, Hokuto Denko).

3 RESULTS AND DISCUSSION

3.1 Electrospun PMMA fibers with $PdCl_2$ particles

Figure 1 (a) and (b) show the optical microscopic (a) and SEM (b) images of the electrospun PMMA fibers with $PdCl_2$ particles. The average diameter of the fibers is 0.67 μm. The fibers have many bead-like structures, their diameter is about 2-5 μm. The beads' size and distribution on the PMMA fibers depended on the electrospinning conditions (applied voltage, distance between the syringe needle and the collector plate), the concentration of the spinning solution, and the loading rate of the electrospinning solution.

Some brown particles are observed in the PMMA fibers as shown in Figure 1 (a). The color of the particles indicates that the particles are attributed to $PdCl_2$.

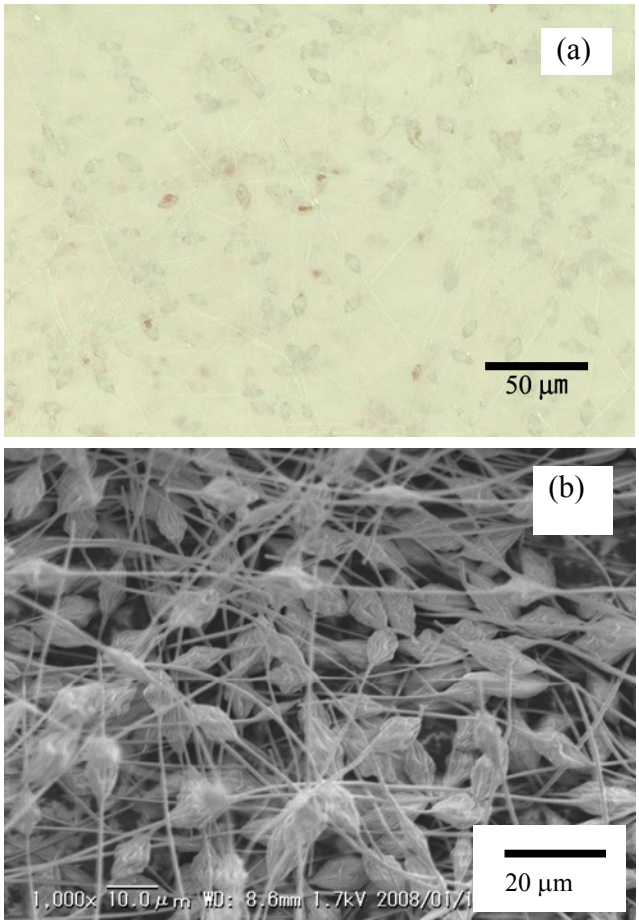

Figure 1 Optical microscope (a) and SEM (b) images of the electrospun PMMA fibers with $PdCl_2$ particles.

3.2 Ni-P plated PMMA fibers

The PMMA mats with $PdCl_2$ were immersed into Ni-P plating bath. The plating rate for the PMMA mats depended on the bath temperature, $PdCl_2$ concentration, and decompression treatment to remove bubbles around the PMMA fibers in the mats. Removing the bubbles around the PMMA fibers was effective to increase in plating rate of and improve homogeneity of the plating layers on the fibers.

Figure 2 shows the SEM image of the Ni-plated PMMA fibers. The sample was plated at 60°C for 60 min. The average diameter of the Ni-plated fibers is 3.0 μm. The thickness of Ni layer on the fiber is about 1.2 μm. XRD patterns of the Ni-plated PMMA mats are shown in Figure 3. The XRD patterns (Figure 3 (b) – (d)) are overlapped with a double-faced adhesive tape for fixing the mats on the

NSTI-Nanotech 2009, www.nsti.org, ISBN 978-1-4398-1784-1 Vol. 3, 2009

sample folder. The peak intensity around at 45° increases in the plating time. This suggests that the peak is attributed to the layer on the PMMA fibers.

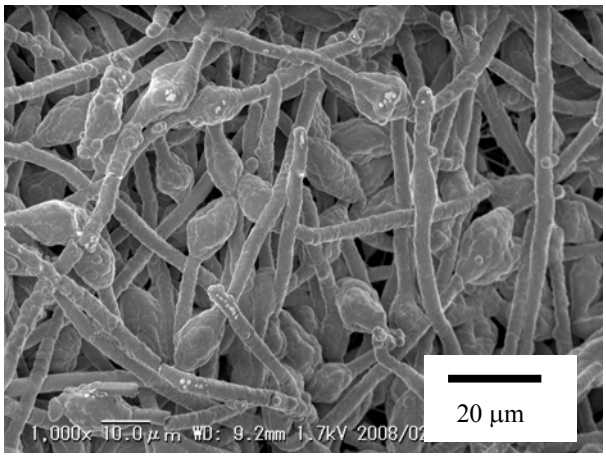

Figure 2 SEM image of Ni-P plated PMMA fibers, plating bath temperature 60°C, plating time 60 min.

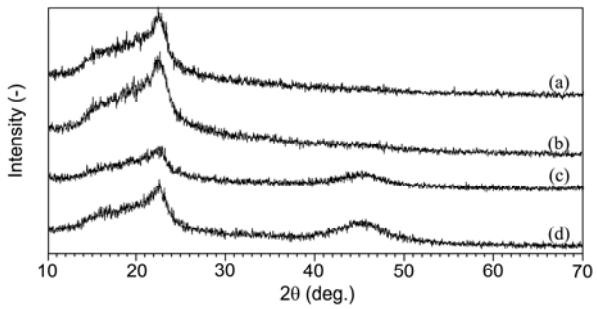

Figure 3 XRD patterns of samples, (a) double-faced adhesive tape, (b) Ni-P plated PMMA fiber, plating time for 30 min, (c) for 60 min, and (d) for 120 min.

Yang *et al.* reported that the peak at 44.1° is attributed to (111) plane of Ni^0 [5]. Therefore, the peak around 45° in Figure 3 indicates that Ni layer grow on the surface of the PMMA fibers.

3.3 Structure of Heat treated Ni-plated PMMA fibers

To estimate optimum heat-treatment temperature for removing the PMMA cores from the Ni-plated fibers, thermogravimetry (TG) analysis was performed. The TG results of the Ni-plated PMMA fibers indicated that the weight loss of the sample starts at 150°C, remarkably occurs at 350 - 400°C. Thermal decomposition behavior of the PMMA fibers agrees with the results in reference [6].

Figure 4 shows the SEM image of heat treated Ni-plated PMMA fibers. As shown in Figure 4, many hollow fibers are observed and it indicates that the PMMA cores in the fibers are removed by the heat treatment at 400°C or 550°C.

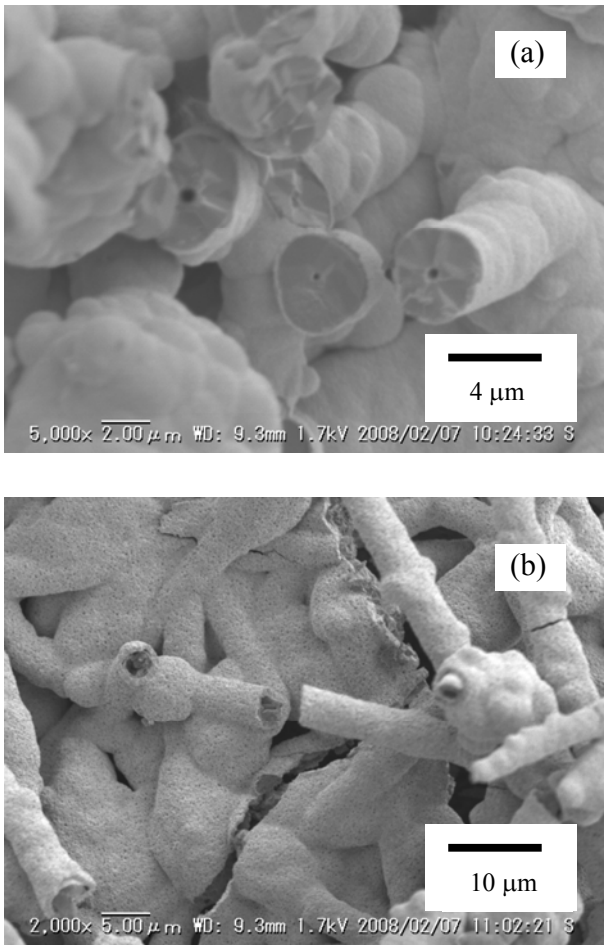

Figure 4 SEM images of heat-treated Ni-plated PMMA fibers, (a) 400°C, 2 h and (b) 550°C, 4 h in the air.

EDX results for heat-treated Ni-plated PMMA fibers (plating condition 60°C, for 60 min) are listed in Table 2. Content of Ni on the PMMA fiber is 75.2 wt. %, P is 4.6 wt. %, O is 7.2 wt. % and C is 13.0 wt. %. According to PMMA structure, the weight ratio of C/O is 1.88. The observed value is 1.81. The value of both agrees approximately. After heat treatment of the Ni-plated fibers in air, the value of C (wt. %) decreases from 13 wt. % to 3.7 wt. % (at 550°C, for 4h). Content of P in the Ni-layers decreased from 4.6 wt. % to 0 wt. % (at 550°C for 4 h). This indicates that P in the plating layer is removed by heat-treatment at 550°C. The theoretical weight ratio of Ni to O (Ni/O) in NiO is 3.67. The observed value of N/O is 5.80 (at 400°C, for 2 h), 4.02 (400°C, 4 h), 1.83 (550°C, 2 h), and 4.15 (550°C, 4h). Increase in heat treatment time and elevation of temperature induce production of NiO by removing P atoms from the plated Ni layers.

Table 2 EDX results of Ni-plated PMMA fibers

Heat-treated temp. (°C)	-	400		550	
Heat-treated time (h)	0	2	4	2	4
C (wt. %)	13.0	15.2	7.5	6.4	3.7
O (wt. %)	7.2	11.9	17.4	32.7	18.7
P (wt. %)	4.6	3.9	5.1	1.0	0.0
Ni (wt. %)	75.2	69.0	70.0	59.9	77.6

Figure 5 shows expanded SEM image of the surface of the heat-treated Ni-plated fibers. Many small pores are observed and roughness of the surface of the Ni-layers increases. Removing P atoms induces the formation of many pores on the surface of the fibers.

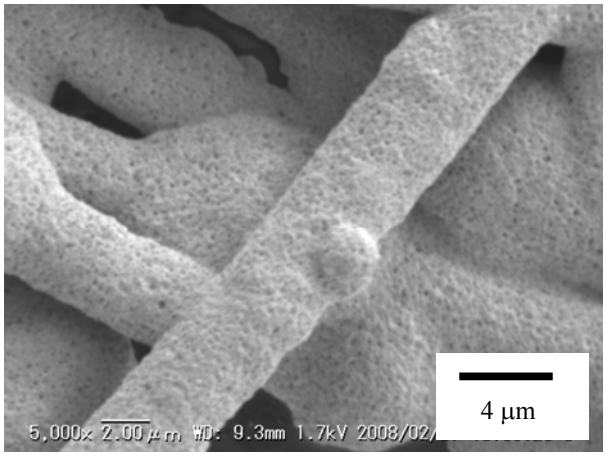

Figure 5 Expanded SEM image of the Ni-plated PMMA fibers, heat treated at 550°C, for 4 h in air.

3.4 Electrochemical behavior of NiO follow fiber electrode in alkali solution

Electrochemical behavior of nickel hydroxide ($Ni(OH)_2$), Ni and Ni-P electrodes have been investigated by many electrochemists with interesting application of these materials to nickel-based secondary batteries, oxygen evolution, organic oxidation. Lo *et al.* have investigated electrochemical behavior of Ni-P plated electrode in alkali solution with surface enhanced Raman spectroscopy.

Figure 6 shows the cyclic voltammograms for the NiO follow fiber electrode in alkali solution (1 M KOH). Anodic and cathodic peaks are observed at 0.44 V and 0.33-0.27 V *vs*. Ag/AgCl. The peaks are attributed to electrochemical reactions as presented in Eq.1 [7].

$$\beta\text{-}Ni(OH)_2 \quad \leftrightarrow \quad \beta\text{-}NiOOH + H^+ + e^- \qquad (1)$$

The theoretical capacity of the reaction is 289 Ah kg^{-1}, 2082 F g^{-1} (charge-discharge voltage range is from 0 V to 0.5 V.). The maximum capacity of the NiO hollow fiber electrode is 190.5 F g^{-1}. The value is higher than that of electrodeposited nano-porous nickel oxide film (167.3 Fg^{-1}) [8].

We concluded that the combination of electrospinning and electroless plating techniques provide simple and unique method for preparation of hollow metal or metal compound nano-fibers. The NiO hollow fiber electrodes prepared by this method have good electrochemical performance.

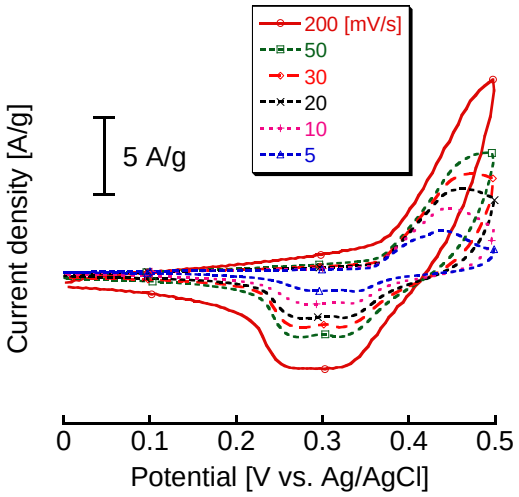

Figure 6 Cyclic voltammograms for NiO follow fibers (heat treated at 550°C for 4 h) electrode in 1M KOH aqueous solution with various scanning rate condition at room temperature.

REFERENCES

[1] B. Dunn, J. W. Long, D. R. Rolison, Interface, 17(3), 49 (2008)

[2] C. R. Martin, Nanomaterials in Li-Ion Battery Research and Development, presented at the International Battery Association Memorial Symposium, Waikoloa, Hawaii, January 7-10, 2003.

[3] S. Ramakrishna, K. Fujihara, W.-E.Teo, T.-C. Lim, Z. Ma, "An Introduction to Electrospinning and Nanofibers", World Scientific Publishing Co., Singapore, 2005.

[4] A. L. Andrady, "Science and Technology of Polymer Nanofibers", A John Wiley & Sons, Inc., U. S. A., 2008.

[5] W. Yang, S. Luo, B. Zhang, Z. Huang, X. Tang, Applied Surface Science, 254, 7427-7430, 2008.

[6] J. E. Brown, T. Kashiwagi, Polymer Degradation and Stability, 52, 1-10, 1996.

[7] Y. L. Lo, B. J. Hwang, Langmuir, 14, 944-950, 1998.

[8] M.-S. Wu,Y.-A. Huang, C.-H.Yang, J.-J. Jow, International Journal of Hydrogen Energy, 32 4153-4159, 2007.